Velocity and Thrust Measurements in a Quasi-Steady Magnetoplasmadynamic Thruster

JAMES M. HOELL JR.,* JOSEPH BURLOCK,* AND OLIN JARRETT JR.*
NASA Langley Research Center, Hampton, Va.

Performance data based on measurements of the average thrust are presented for two repetitively pulsed, gas-fed, quasi-steady MPD arcs having ratios of anode-to-cathode radius of 1.75 and 5.24. An L-C pulse-forming network utilizing electrolytic capacitors is used to form current pulses up to 9000 amps in magnitude and having a flat portion lasting approximately 320 μsec. Ion-collecting probes are used to obtain time-of-flight velocity measurements which correlate moderately well with thrust for some operating conditions. Based on thrust and probe velocity measurements, an apparent limiting specific impulse occurring between 1000 and 1300 sec for both thrusters tested is identified, beyond which erosion or entrainment affects performance. The thrust efficiency at 1300 sec is found to be 15% and 8% for ratios of anode-to-cathode radius of 5.24 and 1.75, respectively.

Introduction

ALTHOUGH the efficiency of steady-state MPD arcs has been observed to increase with power,[1] it has not been possible to examine fully this trend because of the enormous problems associated with operating an arc continuously in the megawatt range where sufficiently high efficiencies are expected. These problems relate primarily to heat transfer to electrodes and mass-flow rate requirements. Of even more concern is the fact that no space-rated power supply capable of producing such powers appears likely for the foreseeable future. Because of this, the quasi-steady mode of operation was welcomed as a method of both simulating the steady-state MPD arc at very high pulsed powers and providing an attractive mode of operation for plasma accelerators. (The reader is referred to Ref. 2 for an extensive bibliography of the work on pulsed devices.) Briefly, the quasi-steady concept requires the application of a current pulse of sufficient duration and magnitude to allow important quantities (current and mass flow) to reach a "steady state." This concept was first applied to MPD arcs when it was realized that a stable and diffuse current pattern could be established in several tens of microseconds in a coaxial configuration.[2] Thus, for properly tailored current pulses, high-peak powers can be maintained at a steady-state condition from which high efficiencies are expected. This feature coupled with the fact that the duty cycle can be set to maintain the input power at a level compatible with present solar power supplies, and the fact that the thrust can be varied with no decrease in efficiency or specific impulse, are the principal attractions of the quasi-steady mode of operation. The disadvantage is, of course, the increased weight and complexity of the power conditioning required to produce extended current pulses, and this may, in fact, prove to be the largest obstacle to be overcome for this approach.

Research groups at Princeton[2-4] and Plasmadyne[5] have operated MPD arcs in a quasi-steady mode. The work by the Princeton group has been primarily concerned with detailed diagnostics which have contributed significantly to the understanding of the quasi-steady process. The work at Plasmadyne has been devoted to the development of an ablation-fed quasi-steady arc and a light-weight pulse-forming network which can readily be used to facilitate thrust measurements. Each effort has provided some performance data which indicate that the quasi-steady MPD arc may indeed outperform its lower-power steady-state counterpart. The performance data in each case, however, have been based on time-of-flight ion velocity measurements of natural disturbances in the arc. This type of measurement gives only the trend of performance since only the local ion velocity is obtained. In this paper, the performance is reported for a repetitively pulsed quasi-steady MPD arc by use of thrust measurements and supporting time-of-flight measurements.

The measurements were obtained for two different accelerators. One was a conventional steady-state MPD arc with an anode-to-cathode radius ratio of 1.75 while the other, with a larger anode orifice, had an anode-to-cathode radius ratio of 5.24. Current pulses with a flat top of about 320 μsec and ranging in magnitude for about 1 ka to 9 ka were produced from an L-C ladder network using low-voltage electrolytic capacitors. The propellant used during these tests was argon. The performance for both geometries was based on measurements of the average thrust at a repetition rate of one pulse per sec. Time-of-flight probe data were found to compare favorably with exhaust velocity derived from thrust and mass flow for some operating conditions. Comparison of time-of-flight and thrust-based velocities lead to the identification of regions of operation for which electrode erosion and entrainment effects are probable.

Quasi-Steady Considerations

The original goal of the quasi-steady concept was to simulate high-power steady-state MPD arc operation without the associated problems of entrainment, erosion, and so forth. Consequently, the quasi-steady mode was subject to a number of rather well-defined restrictions on current, mass flow, and cathode emission. The conditions which have been placed on these parameters for quasi-steady operation are discussed in Ref. 2 and are briefly restated here for interpretation of the results.

Of first concern in obtaining quasi-steady operation is the current distribution which must stabilize to a diffuse quasi-steady pattern. While no direct measurements were made to determine the current distribution, there was indirect evidence of the establishment of a diffuse stable discharge for most of the currents reported here. For example, both the current and voltage traces displayed a steady flat portion

Presented as Paper 70-1080 at the AIAA 8th Electric Propulsion Conference, Stanford, Calif., August 31–September 2, 1970; submitted September 23, 1970; revision received July 9, 1971. The authors wish to express their gratitude to C. B. Karpa and J. A. Williams for their valuable assistance in performing the experiments.

Index category: Electric and Advanced Space Propulsion.

* Aerospace Technologist, Aero-Physics Division. Member AIAA.

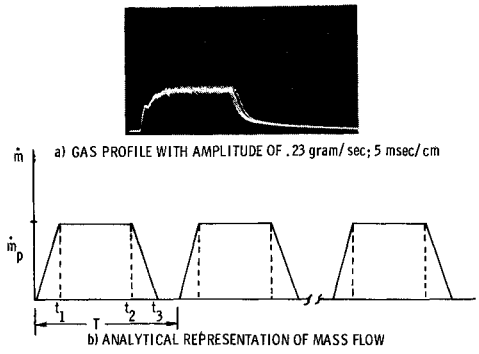

Fig. 1 Typical time history of propellant pulse.

lasting for a significant portion of the entire current pulse. Also, for most of the current levels reported here, the cathode and anode remained free from any signs of localized arc attachment such as pitting. Finally, consider the empirical relationship $t_s \simeq (\frac{1}{2}J)$ sec where t_s is the time required for current stabilization, and J is the pulsed current. In Ref. 2, for a limited range of currents, this relationship was found to provide a measure of the time required for stabilization. If this relation is assumed to hold for the present thrusters then, except for the lowest currents used, t_s is generally less than the rise time of the current pulses.

The propellant flow rate is the next input parameter which must be tailored for quasi-steady operation. First, the mass flow must be of the right order of magnitude. A first-order approximation for the mass-flow rate can be obtained from the self-magnetic force equation [Eq. (3), below] together with an assumed value of specific impulse. For the present experiment, this gives flow rates on the order of a few tenths of a gram per second. For a flight system, it is obvious that the propellant pulse must be coincident with the current pulse. For a laboratory system, a match between the propellant and current pulse is not necessary. The major concern is that the rise time be short enough to avoid a gas buildup in front of the accelerator before initiation of the current pulse, and that the length of the pulse be short enough to avoid too great an increase in pressure during repetitive operation. The propellant should also establish a steady flow during the current pulse. The time scale for this should be on the order of an accelerator dimension divided by the acoustic speed. Typical propellant time profiles are shown in Fig. 1. The rise time of the pulse is approximately 3 msec. While this is longer than desired, it was felt that by initiating the main discharge at the beginning of the flat portion, the effect of gas accumulation in front of the thruster could be minimized to such an extent that the results would not be affected. The flat portion, about 17 msec, was sufficiently short so that the vacuum system could maintain a background pressure of about 10^{-4} torr or better during all the tests reported here.

For simulation of steady MPD arcs as well as for efficient operation of the quasi-steady mode, the cathode emission process should be dominated by thermal emission. This reduces the cathode fall and cathode erosion. The present measurements do not include a determination of the cathode temperature. However, an evidence that thermal emission is the dominant mechanism is the fact that the cathode did not exhibit a sandblast appearance characteristic of cold-cathode operation. In addition, use of a barium-impregnated tungsten cathode should encourage thermionic emission.

Finally, from the studies presented in Ref. 2, it appears that the mass-flow rate must be matched to the arc current for "proper" operation. While this matched flow rate was experimentally determined for the device used in Ref. 2, it was not clear how this should scale to the present engines or, for that matter, if the thrusters used here would exhibit a similar characteristic.

Experimental Apparatus

As indicated above, the requirement on the current pulse for quasi-steady operation is that it be of sufficient duration and magnitude to allow a quasi-steady condition to prevail over a significant portion of the pulse. Such an extended current pulse is best achieved by using a lumped parameter transmission line.

Use of paper capacitors in the construction of a transmission line matched to the arc impedance (about 5 mΩ) would result in weight excessive for the thrust stand. Also, impedance matching transformers used in conjunction with a higher impedance line having smaller capacitor weight become rather large for currents of interest and would be difficult to mount on a thrust stand. In order to avoid the constraints mentioned above, the authors have followed the work of Ducati[5] by using electrolytic capacitors in the construction of a low-voltage, high-capacitance transmission line. It was demonstrated in Ref. 5 that an acceptable waveform could be produced using electrolytics. For the present work, a network with 10 sections, each containing capacitance of 1800 μf each, with the last five sections separated by inductors of 0.25 μh each (shown schematically in Fig. 2) was used. The current and voltage waveforms shown in Figs. 3a and 3b were obtained for the small and large accelerator, respectively. The flat portions are approximately 320 μsec long. The high internal impedance characteristic of the electrolytics is manifested in this figure by the long tail, and during actual operation by a loss of energy in the capacitors (i.e., only about 50% of the stored energy appears across the electrodes).

The lightweight electrolytic network greatly simplifies thrust measurements since both the transmission line and the thruster can be mounted on the thrust stand. This eliminates the need for feeding high-current pulses onto the thrust stand, and consequently the large errors which normally arise from the current leads (i.e., heating, interaction between leads, etc.). In addition, the gas supply was mounted onboard so that the only connections to the thrust stand were two relatively small charging leads, instrumentation leads for monitoring the current and voltage, and signal leads to the gas valve and starter electrode. The thrust stand itself was a seismic pendulum type. It was originally designed for dc operation with manual adjustment to null the thrust-level output. It was found that the mechanical nulling device produced unreliable results in the fractional millipound range. Operating the stand in an open-loop mode (i.e., measuring only the amount of deflection from its natural null portion) gave extremely reproducible results down to a thrust level of about 100 μlb. The magnitude of the deflection from null for a given thrust range (i.e., the sensitivity) was controlled by the tilt of the thrust stand—the greater the tilt angle, the less sensitive the stand and conversely. Furthermore, since the natural period of the thrust stand was determined to be on

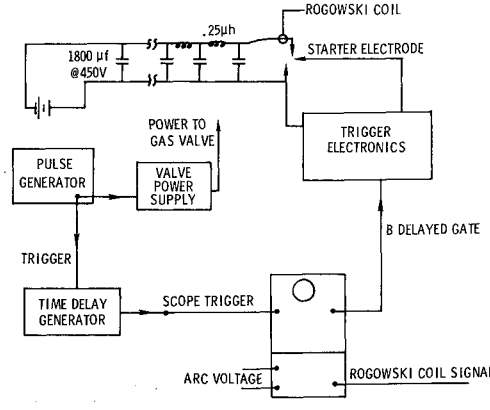

Fig. 2 Schematic quasi-steady electronics.

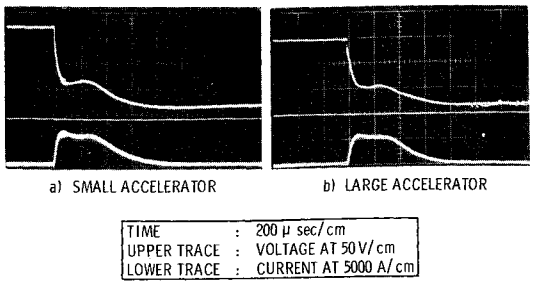

Fig. 3 Current and voltage characteristic for quasi-steady accelerator.

the order of 5–7 sec, the output for load variations of one cycle per sec or greater was an average value. The deflection of the thrust stand was sensed by a linear-variable differential transformer. The output was indicated on an oscillograph recorder. The thrust stand was calibrated by applying known forces to the stand via a friction-free support described in Ref. 6.

A schematic of the two accelerators used during these tests is shown in Figs. 4a and 4b. The one shown in Fig. 4a has a copper-tungsten anode (16% Cu) with a $\frac{7}{8}$-in. i.d. and a barium impregnated tungsten cathode with a $\frac{1}{2}$-in. o.d. The one shown in Fig. 4b has a stainless-steel anode with a 2-$\frac{1}{4}$in. i.d. and a barium impregnated tungsten cathode with an o.d. of $\frac{7}{16}$ in. These two designs give a ratio of anode-to-cathode radius of 1.75 and 5.24, respectively. Each thruster has a starter electrode which was used to initiate the main discharge at the beginning of the flat portion of the gas pulse.

All the tests reported here were conducted in the 13-ft-diam × 21-ft-long vacuum tank at the Langley Research Center. This facility was capable of maintaining a background pressure during these tests of 10^{-4} torr, or less.

Two pairs of floating double probes, each with a 45-volt bias between the probes, were used to obtain time-of-flight ion velocity measurements. A schematic of the probe circuit is shown in Fig. 5. The separation distance between the two double probes was 15 cm. Both were mounted on a mechanical drive so that both an axial and a radial survey could be made.

Propellant pulses were introduced into the thruster via a commercially available solenoid valve. Time-history profiles, shown in Fig. 1a, were obtained using a fast-response millitorr gage. As shown in Fig. 1b, the actual gas pulse can be approximated by a profile which has a linear rise time, a flat portion, and a linear decay. The instantaneous mass flow during the flat portion can then be expressed as

$$\dot{m} = T\langle\dot{m}\rangle/[t_1/2 + (t_2 - t_1) + (t_3 - t_1)/2] \quad (1)$$

where $\langle\dot{m}\rangle$ is the average mass flow for repetitive pulses with a period of T, and t_1, t_2, and t_3 are times indicated on the figure. The average flow rate was measured by using a thermal mass flowmeter. These meters have a long response time compared to the repetition rate used during these tests. Thus, by placing the flowmeter in series with the valve, the average flow rate is read directly. As a check on the response of the meter, the repetition rate was changed from one to two pulses per second. The indicated flow rate showed a proportional increase.

Results and Discussion

Thrust and Probe Measurements

For MPD thrusters operating with arc currents greater than approximately 1 ka and without an external field, the thrust can be attributed to two components—an aerodynamic force due to the heating and expansion of the propellant, and an electromagnetic force due to the interaction of the applied

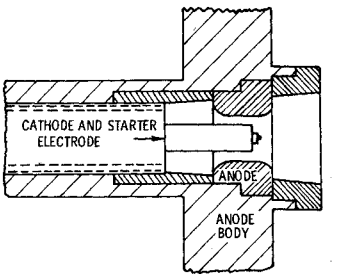

a) Small diameter anode thruster

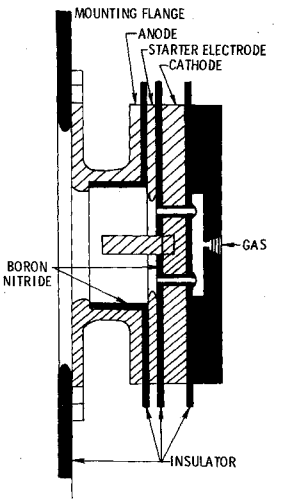

b) Large diameter anode thruster

Fig. 4 Schematic of quasi-steady thrusters.

current with the resulting self-magnetic field. The aerodynamic force has been expressed as

$$F_a = C_f P_0 A_t \quad (2)$$

where A_t is the area of the nozzle throat, C_f is the thrust coefficient, and P_0 is the pressure of the gas in the discharge.[7] The self-magnetic force is given by

$$F_s = \mu_0/4\pi I^2[\ln(r_a/r_c) + 0.75] \quad (3)$$

where I is the applied current, and r_a/r_c is the ratio of the anode-to-cathode current attachment radius.[8]

It should be noted here that for pulsed-operation Eq. (3) gives the peak self-magnetic force rather than the average force measured by the thrust stand. The average theoretical force is obtained by averaging over I^2. Assuming that the major contribution to the thrust originates from the peak current, that is, flat portion of the pulse, the average thrust is given by

$$\langle F_s\rangle = [t_d/T]F_s \quad (4)$$

where t_d is the pulse duration and T is the period. For the measurement reported in this paper, the period is 1 sec and

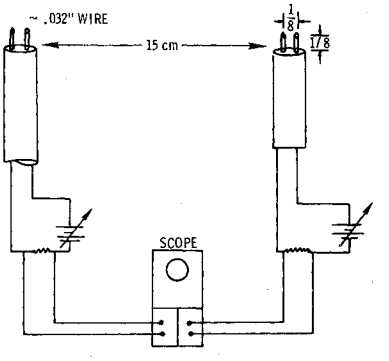

Fig. 5 Double-probe circuit.

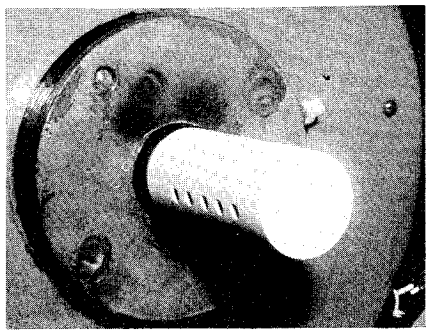

Fig. 6 Thrust killer attached to small orifice accelerator.

the pulse duration has been assumed to be equal to the flat portion of the current pulse, that is, $t_d = 320$ μsec.

Before recording thrust data, a number of tests were performed on the thrust system to determine to what extent tare forces would affect the measurements. The first test consisted of operating the thruster with a thrust killer to determine the effect of the charging current, valve operation, thruster heating, and the main discharge on the output of the thrust stand. The thrust killer was constructed from a boron-nitride cylinder closed at one end with holes drilled radially through it. This was attached to the thruster so that no plasma could escape the thrust system with an axial velocity. Thus, the net force in the thrust direction due to plasma accleration was zero. A photograph of the thrust killer attached to the thruster is shown in Fig. 6. Operation of the thruster with the thrust killer in place produced no detectable deflection from the zero position. The next test was to determine if the time constant of the thrust stand was indeed long enough to give an average value for pulsed operation at the lowest repetition rate used during these tests. This was done by observing the output as one pulse per sec and then at two per sec. It was found that to within 10% the output doubled, indicating that the pulsed thrust is effectively averaged. Next, to determine if the elasticity of the brackets connecting the thruster to the thrust stand might introduce an error, a pulsed load was applied to the thrust stand first via the thruster and then directly. This was done by attaching a metal washer to the thruster and then pulsing a solenoid placed close to the washer. The washer was then attached to the thrust stand directly. The output for each washer position agreed to within 20%. Considering the crudeness of the test arrangement, this agreement is considered good. To check on the possibility of a portion of the pulsed gas circulating to the rear of the thruster, striking the thruster, causing a negative thrust, the following test was performed. The gas valve was disconnected from the thrust system and placed in front of the anode so that the gas-flow conditions during operation could be approximated. The gas valve was operated at one pulse per sec and the output from the thrust stand was monitored. There was no detectable

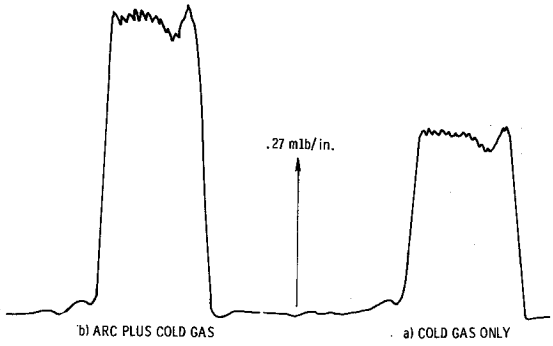

Fig. 7 Thrust stand output due to cold gas and arc plus cold gas.

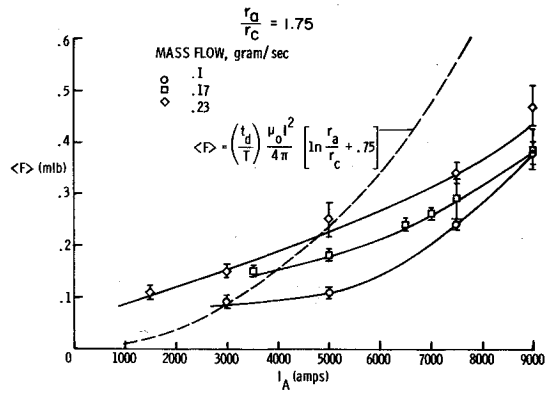

Fig. 8 Average thrust vs arc current for thruster with $r_a/r_c = 1.75$.

deviation from the zero thrust position. The final test consisted of determining the tare force due to the cold gas flow, and, in particular, of determining its magnitude as compared to the force due to cold gas plus the arc. The output due to cold gas flow is compared to the output due to cold gas plus plasma flow in Fig. 7. It can be seen that while the gas pulse represents a sizable portion of the total output, the thrust due to the arc can be determined without any difficulty. The amplitude of the gas pulse for these tests is determined to a large extent by its length. For a flight system, the gas pulse would contribute to the thrust but, since it would presumably be matched to the current pulse, it would be a small contribution. Consequently, only the difference between these traces is reported here.

Figure 8 displays the dependence of thrust on the current and propellant flow rate for the small orifice thruster. The shot-to-shot reproducibility of the data was quite good as indicated by the error bars. The solid lines represent a least-square fit to the experimental data. The dashed curve is the averaged theoretical thrust calculated from Eq. (4) using the appropriate value for r_a/r_c. The important fact about this figure is that for a constant mass flow the thrust has only a weak dependence on the current. This, together with the variation of thrust with mass flow, indicates that for this thruster the self-magnetic force, given by Eq. (3), is only weakly felt.

Consider now the results of the time-of-flight velocity measurements obtained for the present thruster. The probe circuit used for these measurements has been described above and was shown in Fig. 5. Typical probe traces for the small orifice device are shown in Fig. 9a for the forward probe 51 cm downstream of the accelerator and with a distance of 15 cm between the probes. The relatively long flat portion is associated with the quasi-steady portion of the thruster operation. In this portion of the probe traces, the fluctuations maintain their identity as the plasma travels from the front probe to the rear one. Readings were made by physical overlay of the traces, noting the displacement required to match the fluctuation structure of the two traces. The time displacement between identical fluctuations was measured and a time-of-flight velocity determined. For the traces shown in Fig. 9a the velocity is approximately 1.9×10^4 m/sec. Using this tech-

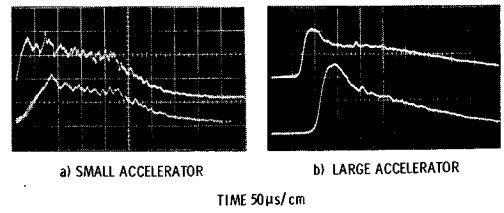

Fig. 9 Double-probe characteristics for small and large quasi-steady thruster.

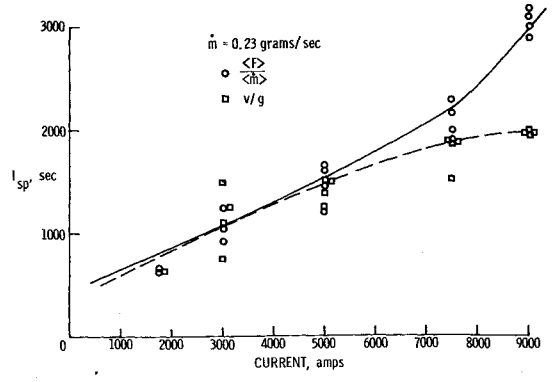

Fig. 10 Comparison of time-of-flight probe data with thrust data for thruster with $r_a/r_c = 1.75$.

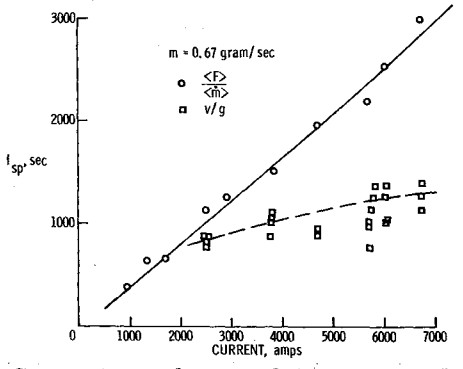

Fig. 12 Comparison of time-of-flight probe data with thrust data for thruster with $r_a/r_c = 5.24$.

nique, the center-line velocity was obtained for the same conditions as for the upper curve of Fig. 8. In Fig. 10, the specific impulse based on probe data is compared to that derived from thrust measurements. These data show good agreement between probe and thrust data up to about 4000 amps or a specific impulse of 1300 sec. At this point, the probe data tend to level off while the thrust data continue to rise. The behavior of these probe data is similar to that observed by the Princeton group when operating with less than their matched mass-flow rate, and can be attributed to an increase in the propellant flow rate over and above that injected by the valve.

Thrust measurements were also made on an accelerator with a larger anode orifice. This thruster (described above) is, in effect, a smaller version of the Princeton device. Figure 11 shows the dependence of thrust on current for two mass-flow rates. The solid line through the experimental points represents a least-squares fit to the data. The dashed curve is the average theoretical thrust computed from Eq. (4) with $r_a/r_c = 5.24$. The data in this figure differ from that in Fig. 8 in that the thrust has a stronger dependence on the current and is always greater than the theoretical thrust by approximately a constant.

Consider again the results of time-of-flight velocity measurements. The same probe circuit described previously was used. Typical probe characteristics are shown in Fig. 9b. Notice that unlike the probe traces obtained from the small accelerator (Fig. 9a), the data from the large device exhibit very few well-defined fluctuations. For this reason, these probe data are felt to be somewhat less reliable than that shown previously. Figure 12 compares, for the same conditions as that for the upper curve of Fig. 11, the specific impulse derived from centerline velocity measurements with that derived from thrust data. In a manner similar to that for the small accelerator, the probe data tend to level off while the thrust data continue to rise. Here, again, the discrepancy between the two sets of data can be attributed to an increase in $\dot{m}$ over that injected by the valve.

Thus, based on probe data, the large accelerator exhibits a characteristic similar to the smaller device described here and the device described in Ref. 2 in that for a given mass flow each exhibits a limiting specific impulse. The limiting value for the large thruster here is not as clearly defined, but seems to be about 1000 sec.

It is interesting that both accelerators exhibit a phenomenon that can be attributed to an onset of erosion or entrainment. Because of the limited range of data presented here, one hesitates to generalize or attribute too great a significance to this, although, as just pointed out, similar results have been observed by Princeton prior to the present work, and also by AVCO more recently.[9] Both groups have determined that for a given propellant and geometry, the parameter $J^2/\dot{m}$ (J = arc current and $\dot{m}$ = propellant flow rate) reaches a critical value which, if exceeded either by an increase in current or a decrease in mass flow, results in a significant increase in erosion from electrodes or insulators. It is felt that the apparent onset of injection of extra mass is related to exceeding the critical value of $J^2/\dot{m}$ for the two accelerators tested.

Thrust Efficiency

Aside from the fundamental interest of the matched mass flow, this aspect of the operation of the thruster is of considerable importance for the interpretation of performance data. The identification of the matched condition, or for the present discussion, the starved flow region, allows one to specify a region of operation where performance data are questionable. From the probe data which were presented in Figs. 10 and 12, the upper limit on the specific impulse for the devices tested here appears to be between 1000 and 1300 sec. Accordingly, we have used 1300 sec as the value beyond which performance data for both thrusters are probably affected by erosion or entrainment. Figure 13 displays the thrust effi-

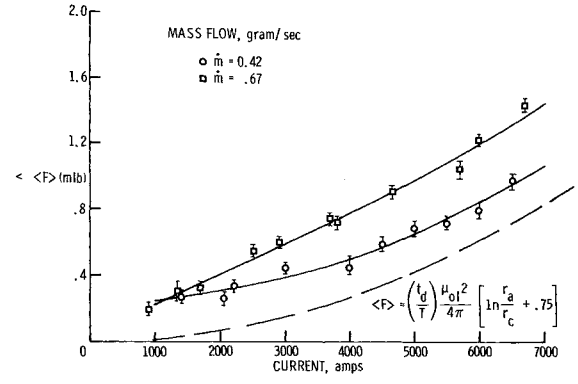

Fig. 11 Average thrust vs arc current for thruster with $r_a/r_c = 5.24$.

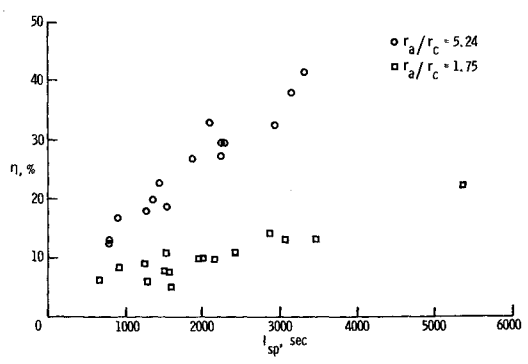

Fig. 13 Thrust efficiency vs specific impulse for small and large anode orifice thruster.

ciency as a function of specific impulse for both devices. The expression for the thrust efficiency is given by

$$\eta = [\langle F \rangle]^2/2\dot{m}P[t_d/T]^2 \quad (5)$$

where $\langle F \rangle$ is the measured thrust, $\dot{m}$ and P are the peak mass flow and arc power, respectively, and the factor t_d/T accounts for the duty cycle. Remembering that 1300 sec is probably the limiting specific impulse, the maximum efficiency that can be considered valid in this figure is 8% for the small engine and 15% for the large engine.

The factor of about 1.9 difference between the two accelerators tested here cannot be attributed entirely to the increase in r_a/r_c [Eq. (3)]. Since at constant I_{sp} the power to each thruster is approximately equal, a comparison of the expected efficiency between the two devices can be obtained by comparing the self-magnetic thrust equations at a given I_{sp}. This gives the ratio of the efficiency for the small accelerator to that for the large accelerator a value of about 1.3 as compared to the 1.9 experimentally measured.

Reference 10 may offer a possible explanation for the difference in performance of the two thrusters. In this reference, potential measurements obtained in a quasi-steady arc with an anode diameter of 4 in. were reported. These measurements indicated that a major portion of the energy was deposited in a region surrounding the cathode, and consequently it was asserted that this region may play an important, though not fully understood, role in the acceleration of the gas. The small gap between the anode and cathode in the low-efficiency engine may tend to inhibit the development of this region, while for the larger device reported here, as in Ref. 10, the full advantages of the cathode envelope may be achieved.

References

[1] Nerheim, N. M. and Kelly, A. J., "Critical Review of the Magnetoplasmadynamic (MPD) Thruster for Space Applications," TR 32-1196, Feb. 15, 1968, Jet Propulsion Lab., Pasadena, Calif.

[2] Clark, K. E., "Quasi-Steady Plasma Accelerator," Rept. 859, May 1969, Dept. of Aerospace and Mechanical Sciences, Princeton Univ., Princeton, N. J.

[3] Clark, K. E. and Jahn, R. G., "Quasi-Steady Plasma Acceleration," AIAA Paper 69-267, Williamsburg, Va., 1969.

[4] Jahn, R. G., Clark, K. E., Oberth, R. C., and Turon, P. J., "Acceleration Patterns in Quasi-Steady MPD Arcs," AIAA Paper 70-165, New York, 1970.

[5] Ducati, C. A. and Jahn, R. G., "Repetitively-Pulsed Quasi-Steady Vacuum MPD Arc," AIAA Paper 70-167, New York, 1970.

[6] Fowke, J. G., "A Three-Component Wind-Tunnel Balance for Measuring Extremely Small Forces," Presented at the ISA National Conference, Houston, Texas, Oct. 27–30, 1967.

[7] Malliaris, A. C., "Plasma Acceleration in an Electric Discharge by the Self-Induced Magnetic Field," *Journal of Applied Physics*, Vol. 38, No. 9, Aug. 1967, pp. 3611–3619.

[8] Jahn, R. G., *Physics of Electric Propulsion*, McGraw-Hill, New York, 1968, Chap. 8.

[9] Malliaris, A. C., John, R. R. Garrison, R. L., and Libby, D. R., "Performance of Quasi-Steady MPD Thrusters at High Powers," private communication, Space Systems Div., Avco Corp., Wilmington, Mass.

[10] Jahn, R. G. et al., "Pulsed Electromagnetic Gas Acceleration," Rept. 634n, Jan. 1, 1970, Princeton Univ.